Self-Calibration Phase-Shifting Digital Holographic Microscopy Based on Carrier Frequency Analysis

Xu Zhennan[1,2] Zhong Jingang[1,2]

[1] *Department of Optoelectronic Engineering, Jinan University, Guangzhou, Guangdong* 510632, *China*
[2] *Key Laboratory of Optoelectronic Information and Sensing Technologies of Guangdong Higher Education Institutes, Guangzhou, Guangdong* 510632, *China*

Abstract Small phase shift errors in phase-shifting digital holographic microscopy can cause distinct errors in wave-front reconstruction. Phase shift errors generally fall into two categories: numerical errors and uneven errors. A considerable numerical error results from miscalibration of phase shifter and ambient vibrations. Therefore, self-calibration phase-shifting scheme is worth trying. Here, a carrier frequency analysis based self-calibration phase-shifting digital holographic microscopy (PSDHM) is proposed. The actual phase shifts are calculated from Fourier analysis of holograms. The uneven errors are caused by irrational configuration of interferometer. We propose an improved Linik interferometer based setup of phase-shifting digital holography. The experimental results certify that both the self-calibration phase-shifting scheme and the proposed experimental setup have a better reconstruction quality.

Key words holography; digital holography; holographic interferometry; phase measurement; interference microscopy

OCIS codes 090.1995; 090.2880; 120.5050; 180.3170

基于载频条纹分析的自定标相移数字全息显微术

徐振南[1,2] 钟金钢[1,2]

[1] 暨南大学光电工程系, 广东 广州 510632
[2] 光电信息传感技术广东省普通高校重点实验室, 广东 广州 510632

摘要 相移误差在很大程度上影响着相移数字显微全息的测量精度。相移误差可大致分为数值误差和不均匀误差两类。相移器的标定错误和环境震动都能产生不可忽略的数值误差,因此自定标相移数字全息是值得探究的。提出了一种基于载频条纹分析方法的自定标相移数字全息显微术。利用傅里叶条纹解调分析方法,分别提取四幅全息图的载频条纹相位。通过对比载频条纹相位获得全息图间的相移量。实验装置设计的不合理导致了不均匀误差。提出一种基于改进型 Linik 干涉仪的相移数字全息显微装置。实验结果证明了自定标算法和改进型的 Linik 干涉仪具有更好的重建结果。

关键词 全息;数字全息;全息干涉仪;相位测量;干涉显微镜

中图分类号 O438.1 **文献标识码** A **doi**: 10.3788/CJL201340.1209001

1 Introduction

Digital holography takes advantage of electronic imaging devices to record holograms, and numerically reconstructs wave-fronts according to holography principle by computer. It has achieved wide use in various fields, such as biomedicine, topography and deformation measurement[1-3]. In recent years, since the surface characteristics of microstructure devices, for example semiconductor chip, affect their properties directly, measurement of surface characteristics of micro structure devices is a significant work. Digital holographic microscopy (DHM) has the advantages of three-dimensional (3D) measurement over traditional measuring methods. Moreover, most of microstructure

收稿日期: 2013-06-20; **收到修改稿日期**: 2013-07-30

基金项目: 国家自然科学基金(61077003.)

作者简介: 徐振南(1989—),男,硕士研究生,主要从事数字全息方面的研究。E-mail: paiqiu5@126.com

导师简介: 钟金钢(1964—),男,博士,教授,主要从事数字全息方面的研究。E-mail: tzjg@jnu.edu.cn(通信联系人)

devices are opaque, so reflective digital holographic microscopy (RDHM) is a good mean of detecting surface characteristics of micro structure devices. Charrière *et al*.[4-5] proposed a Mach-Zehnder (M-Z) interferometer-based reflective off-axis Fresnel digital holographic microscopy. Compared with reflective off-axis Fresnel digital holography, reflective phase-shifting digital holography (PSDH) has a better performance in suppressing zero-order diffraction and twin image terms in wave-front reconstruction.

Generally, PSDH needs acquiring no less than three holograms with different phases. The phase differences are introduced by phase shifter. The accuracy of phase shifts has significant influences upon reconstruction quality. Phase shift errors usually fall into two categories: uneven errors and numerical errors. The former is caused by irrational configuration of interferometer. The latter results from miscalibration of phase shifter and ambient vibrations. So far, various methods to deal with numerical errors have been developed. Kong *et al*.[6] proposed a general iterative least-squares (ILS) method, which consists of two iterative fitting procedures: a linear serial least-squares fitting and a nonlinear spatial least-squares fitting. Then it is simplified through substituting a linear minimization procedure for the nonlinear spatial least-squares fitting[7], and simulations prove it to be feasible. Recently, an iteration based self-calibration PSDH is presented by Vargas *et al*.[8]. Both translational and inclined deviations of reference mirror and even the vibrations of camera are taken into account. In their method, the phase shifts are introduced by ambient vibrations. However, iterative methods easily subject to substantial computational burden.

A phase shift determination method in point-diffraction interferometer [named as Fourier-transform phase-shift determination (FTPSD)] is presented by Goldberg *et al*.[9]. FTPSD method obtains phase shifts through extracting the phase of the maximum point of +1 order spectrum in frequency domain, which has less computational burden than ILS. In this paper, we propose a self-calibration reflective phase-shifting digital holographic microscopy (PSDHM) by combining improved Linik interferometer and FTPSD method. The improved Linik interferometer can minimize uneven errors effectively. Four carrier-frequency holograms with different phases are recorded in off-axis holography. And their carrier frequency phase differences can be approximated as phase shifts. The approximation is well established when holograms' Fourier spectra are separated adequately. The experimental results indicate that self-calibration four-step phase-shifting scheme has a better performance in wave-front reconstruction than traditional four-step phase shifting holography.

2 Phase-shifting digital holography and improved Linik interferometer

Zhang *et al*.[10-11] presented the in-line PSDH. The holograms are formed by interference of reflected beam from object and reference beam. Assuming that N phase steps are finished, the camera records $N+1$ holograms. The interference intensity distribution of the nth ($n=0,1,\cdots,N-1,N$) hologram is

$$I_n = |E_R|^2 + |E_O|^2 + 2|E_O||E_R|\cos(\phi+\alpha_n), \tag{1}$$

where E_O and E_R are complex amplitudes corresponding to object and reference waves, ϕ represents the interference phase, and α_n denotes the phase shift between I_n and I_0. I_0 is the first hologram without phase step, and $\alpha_0 = 0$. There are three unknowns in Eq. (1), while I_n and α_n are prior known. Assuming that phase shifts are global and arbitrary, in order to obtain ϕ, at least three holograms are needed. We can derive the complex field $E_0 = |E_0|\exp(j\phi)$ on the sensing plane of camera, where the phase of the complex field is expressed by four holograms as

$$\phi = \arctan\frac{(I_0-I_2)(\cos\alpha_3-\cos\alpha_1)-(I_3-I_1)(1-\cos\alpha_2)}{(I_0-I_2)(\sin\alpha_3-\sin\alpha_1)+(I_3-I_1)\sin\alpha_2}. \tag{2}$$

And the complex field is given by

$$E_O = \frac{1}{2|E_R|}\frac{(I_0-I_2)+j(I_3-I_1)}{[\cos\phi-\cos(\phi+\alpha_2)]+j[\cos(\phi+\alpha_3)-\cos(\phi+\alpha_1)]}. \tag{3}$$

Then holographic reconstruction can be done by performing Fresnel diffraction or angular diffraction of E_O through a reconstruction distance d_0. Since the proposed reflective PSDHM is imaging plane holography, angular spectrum diffraction is adopted:

$$E'(x,y) = \left(\frac{1}{2\pi}\right)^2\iint_{\Sigma_0}dk_x dk_y \exp(jd_0\sqrt{k^2-k_x^2-k_y^2})\iint_{\Sigma_0}d\xi d\eta E_O(\xi,\eta), \tag{4}$$

Where (x,y) and (ξ,η) are the coordinate of reconstruction plane and hologram plane, respectively, and Σ_0 is the sensing area of camera. There are two main issues for achieving high reconstruction resolution: firstly, phase shifts are assumed as global; secondly, phase shifts α_n should be prior known accurately. The first problem is settled by adding a lens L3 in traditional Linik interferometer setup (as shown

in Fig. 1), and the new configuration is called as improved Linik interferometer. In the improved Linik interferometer, L1, L2 and L3 represent lenses, BS is the beam splitter, MO1 and MO2 are objectives, M is the holophote, PZT is the piezoelectric transducer and the incident wave on the reference plane is plane wave, which can avoid the uneven phase shift errors caused by traditional Linik interferometer.

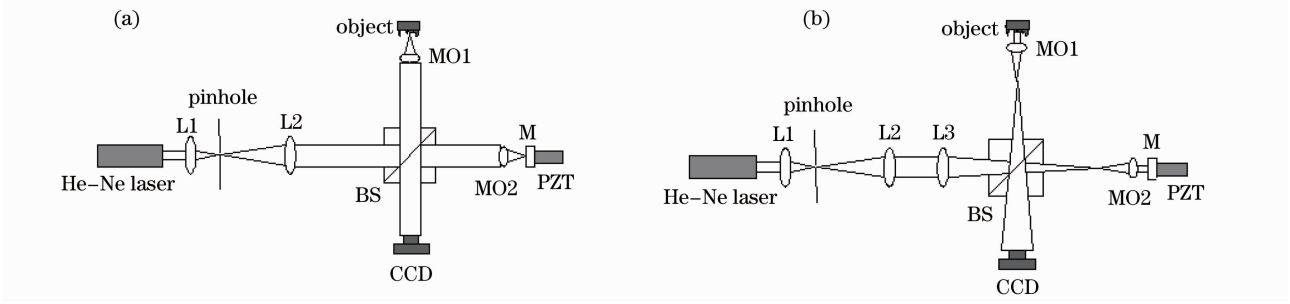

Fig. 1 Interferometer configurations for digital holographic microscopy. (a) Traditional Linik interferometer; (b) improved Linik interferometer

3 Determination of arbitrary phase shift

Generally, phase shifts are calibrated by phase shifter. In traditional four-step phase-shifting holography, phase shifts are $\frac{n\pi}{2}$. However, accurate calibration of phase shifter is hard and interference fringes are so sensitive to vibratory disturbances that actual phase shifts always differ from calibrated ones, which means that the phase shifts are still unknown. In this paper, a carrier frequency analysis method is performed to extract actual phase shifts from interference fringes. The intensity distribution of the nth hologram should include a carrier frequency term, which is expressed as

$$I_n(x,y) = A(x,y) + B(x,y)\cos[\varphi(x,y) + 2\pi(xf_{0x} + yf_{0y}) + \delta_n], \tag{5}$$

where $A(x,y)$ and $B(x,y)$ are equal to $|E_O|^2 + |E_R|^2$ and $2|E_O||E_R|$ in Eq. (1), respectively; f_{0x}, f_{0y} are the fundamental frequencies; δ_n is the additional phase introduced by reference wave, which changes among different holograms. For convenience, we replace the cosine function in Eq. (5) with imaginary exponentials. So intensity distribution of the nth hologram can be expressed as

$$I_n(x,y) = A(x,y) + \frac{1}{2}C(x,y)\exp[\mathrm{j}2\pi(xf_{0x} + yf_{0y})]\exp(\mathrm{j}\delta_n) + \frac{1}{2}C^*(x,y)\exp[-\mathrm{j}2\pi(xf_{0x} + yf_{0y})]\exp(-\mathrm{j}\delta_n), \tag{6}$$

where $C(x,y) = B(x,y)\exp[\mathrm{j}\phi(x,y)]$, and C^* is the complex conjugate of C. The first item in the right of Eq. (6) corresponds to the zero-order diffraction, while the last two ones correspond to twin image terms. Its Fourier transform is

$$F_n(f_x,f_y) = a(f_x,f_y) + \exp(\mathrm{j}\delta_n)c(f_x - f_{0x}, f_y - f_{0y}) + \exp(-\mathrm{j}\delta_n)c^*(f_x + f_{0x}, f_y + f_{0y}), \tag{7}$$

where $a(f_x,f_y)$ and $c(f_x,f_y)$ are the Fourier transforms of $A(x,y)$ and $C(x,y)$. Typically, $a(f_x,f_y)$ and $c(f_x,f_y)$ are both strongly peaked at zero frequency. At the location of (f_{0x},f_{0y}) in frequency domain, an approximation is made as

$$F_n(f_{0x},f_{0y}) = a(f_{0x},f_{0y}) + \exp(\mathrm{j}\delta_n)c(0,0) + \exp(-\mathrm{j}\delta_n)c^*(2f_{0x},2f_{0y}) \approx \exp(\mathrm{j}\delta_n)c(0,0), \tag{8}$$

where, $c(0,0)$ is a complex constant coefficient for all holograms. $F_n(f_x,f_y)$ multiplies a mask matrix $\boldsymbol{M}$, which is a matrix with the same size as hologram including zero elements except that the element corresponding to the maximum point of Fourier spectrum is equal to 1. That is, $\boldsymbol{F}_{nM}(f_{0x},f_{0y}) = F_n(f_x,f_y)\cdot\boldsymbol{M}$. Then by applying the operation of inverse Fourier transform and inverse tangent to $\boldsymbol{F}_{nM}(f_{0x},f_{0y})$, we can obtain

$$\delta_n + P = \arctan\{\mathscr{F}^{-1}[\boldsymbol{F}_{nM}(f_{0x},f_{0y})]\}, \tag{9}$$

where P is a constant. Therefore, after introducing a constant phase offset, the actual phase shift between the nth hologram and the first one is

$$\alpha_n = \delta_n - \delta_0 = \arctan\{\mathscr{F}^{-1}[\boldsymbol{F}_{nM}(f_{0x},f_{0y})]\} - \arctan\{\mathscr{F}^{-1}[\boldsymbol{F}_{0M}(f_{0x},f_{0y})]\}. \tag{10}$$

Then combined with Eqs. (2) - (3), the numerical reconstruction is done. It is important to note that the phase of complex field contains carrier frequency term, which leads to slant phase distribution. By means of eliminating carrier frequency, we can get smooth phase distribution.

The Fourier transform analysis has inevitable errors too, which mostly result from two reasons: firstly, a discrete error exists when finding the location of (f_{0x}, f_{0y}) in Fourier spectrum; secondly, the approximation of Eq. (8) has limitations. The approximation is well established when zero diffraction and twin image contribute little to the spot of (f_{0x}, f_{0y}) in Fourier spectrum.

4 Experimental results

The experimental setup of self-calibration reflective PSDHM is shown in Fig. 1 (b). In experiment, the light source is a He-Ne laser with wavelength of 632.8 nm. A PZT controlled by computer drives the mirror M to generate the phase shifts. A calibrated error, which is same in each step, is introduced by setting PZT parameters artificially, and then four holograms (illustrated in Fig. 2) are recorded by a camera with 1312 pixel × 1082 pixel resolution of 8.0 μm × 8.0 μm pixel size. The sample is USAF-1951 resolution target. Because both semiconductor chip and the resolution target are common for flat substrate, the resolution target is an excellent sample for testing imaging quality. MO1 and MO2 shown in Fig. 1(b) are 4× objectives with numerical aperture (NA) of 0.1. For convenience of numerical reconstruction, the holograms are truncated to be 512 pixel × 512 pixel.

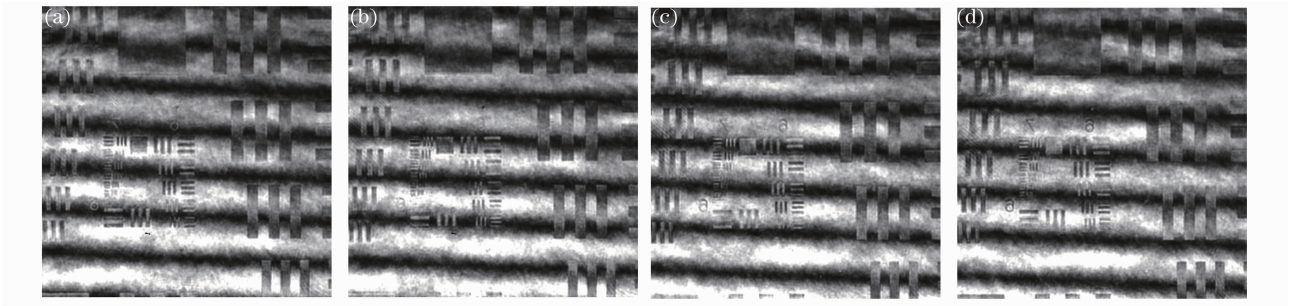

Fig. 2 Four holograms acquired by camera

According to the method mentioned above, we apply the operation of mask to Fourier spectrum of the holograms to obtain the item of $\boldsymbol{F}_{nM}(f_{0x}, f_{0y})$. Then inverse Fourier transform and inverse tangent are done and the wrapped phase of carrier frequency is obtained. Figure 3 shows the Fourier transform analysis results of the hologram shown in Fig. 2(a). The four holograms' wrapped carrier frequency phases are illustrated in Fig. 4. Table 1 lists the calculated phase shifts α''_n by self-calibration algorithm. For convenience, we take $\alpha'_n = \frac{n\pi}{2}$ (named as traditional phase shifts) for comparison. And ε_n is the difference by subtracting the traditional phase shift from calculated one.

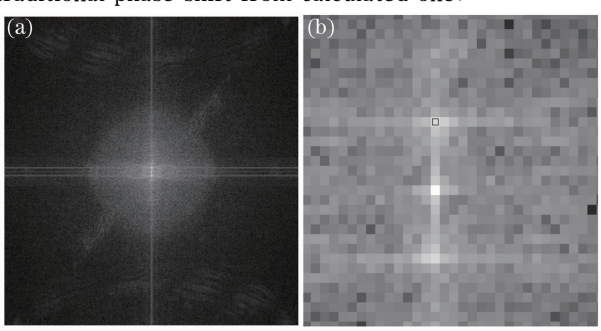

Fig. 3 Carrier frequency analysis of hologram. (a) Fourier spectrum of the hologram; (b) amplification of the Fourier spectrum in which the point in black rectangular is the maximum point of +1 order Fourier spectrum

Table 1 Comparison between traditional and calculated phase shifts (unit: rad)

Phase shift	Traditional value α'_n	Calculated value α''_n	Difference $\alpha''_n - \alpha'_n$
α_1	$-\pi/2$	−1.1641	$\varepsilon_1 = 0.40665$
α_2	$-\pi$	−2.1767	$\varepsilon_2 = 0.96480$
α_3	$-3\pi/2$	−3.1934	$\varepsilon_3 = 1.51885$

From Table 1, it is clear that the calculated phase shifts have big differences from traditional ones. The differences contain calibrated error as well as vibration errors, so we denote the difference as $\varepsilon_n = \varepsilon_{vn} + \varepsilon_{cn}$, where ε_{vn} is vibration error and ε_{cn} is calibrated error. Since calibrated error is equally spaced, the difference can be rewritten as $\varepsilon_n = \varepsilon_{vn} + n\varepsilon_{c0}$, and ε_{c0} is the introduced calibrated error in each step. That is the reason why the differences in Table 1 increase with phase steps. Moreover, the vibration error is random, so increments of the differences are not equivalent. The reconstructed results are illustrated in Fig. 5. Because the sensing plane of camera is located in image plane approximately, the angular spectrum diffraction can be neglected. The wrapped phase of complex field contains a carrier frequency item, which leads to the slant unwrapped phase distribution [Fig. 5(b)]. By eliminating carrier frequency, the smooth unwrapped phase distribution and its expression in three dimensions shown in Figs. 5(c) and (d) are obtained.

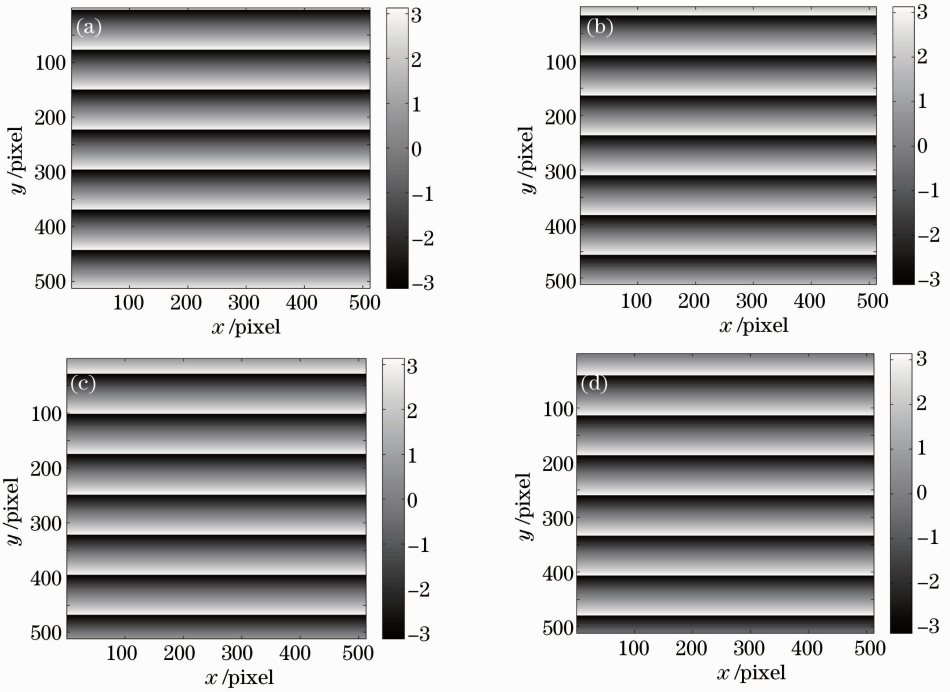

Fig. 4 Carrier frequency phase distribution of the four holograms

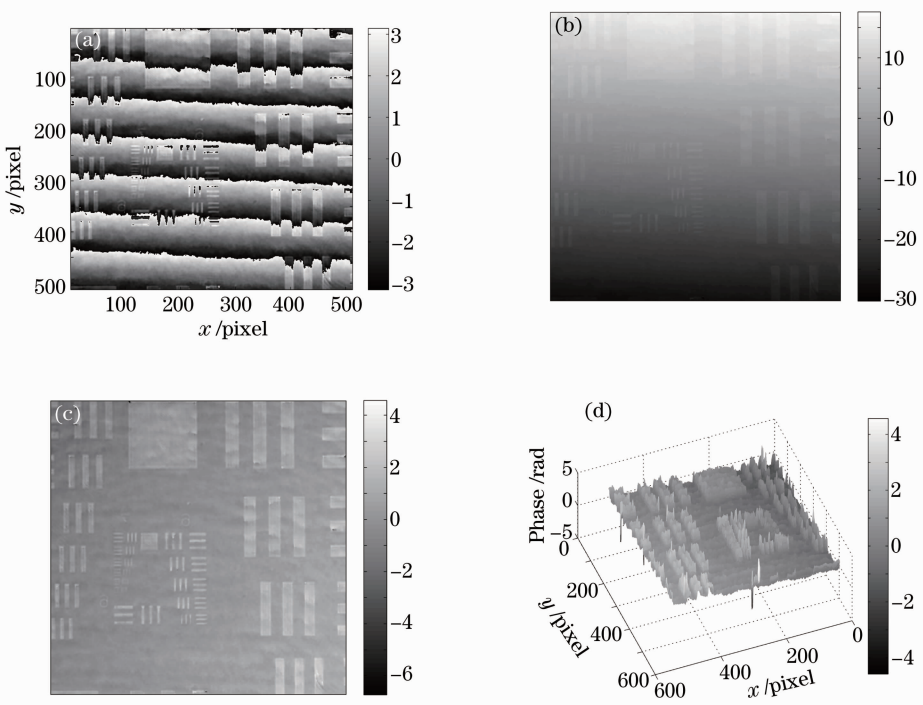

Fig. 5 Wave-front phase distribution reconstruction results. (a) Wrapped wave-front phase distribution; (b) slant unwrapped wave-front phase distribution; (c) smooth unwrapped wave-front phase distribution; (d) three-dimensional expression of Fig. (c)

In order to show the improvement of the self-calibration algorithm effectively, a reconstruction quality evaluation method[12] is applied. Because deviations of phase shifts affect the reconstructed wave-front intensity distribution straightly, the correlation coefficient between the reconstructed intensity distribution and the recorded one can reflect the reconstruction quality. And the larger the correlation coefficient is, the better the quality is. Correlation coefficient is expressed as

$$\rho = V_C(I_{cal}, I_O) / \sqrt{D_{I_{cal}} D_{I_O}}, \tag{11}$$

where V_C and D represent covariance and variance, respectively; I_O, I_{cal} are the recorded intensity

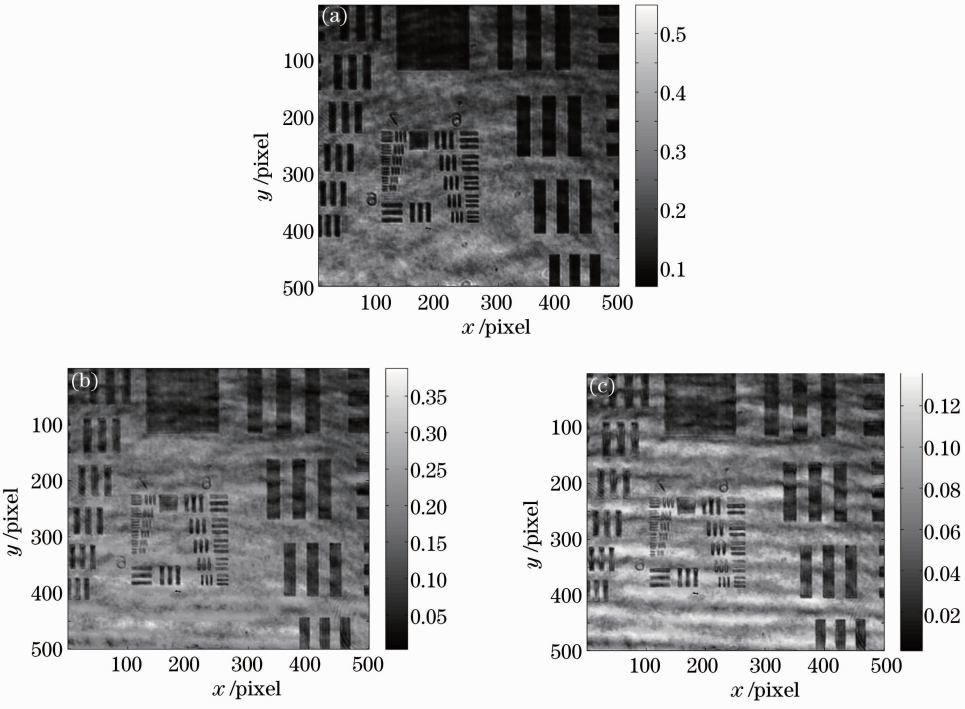

Fig. 6 Wave-front intensity distribution. (a) Recorded intensity distribution of object wave with blocking the reference beam; (b) reconstructed intensity distribution of object wave with extracted phase shifts; (c) reconstructed intensity distribution of object wave with incorrect phase shifts

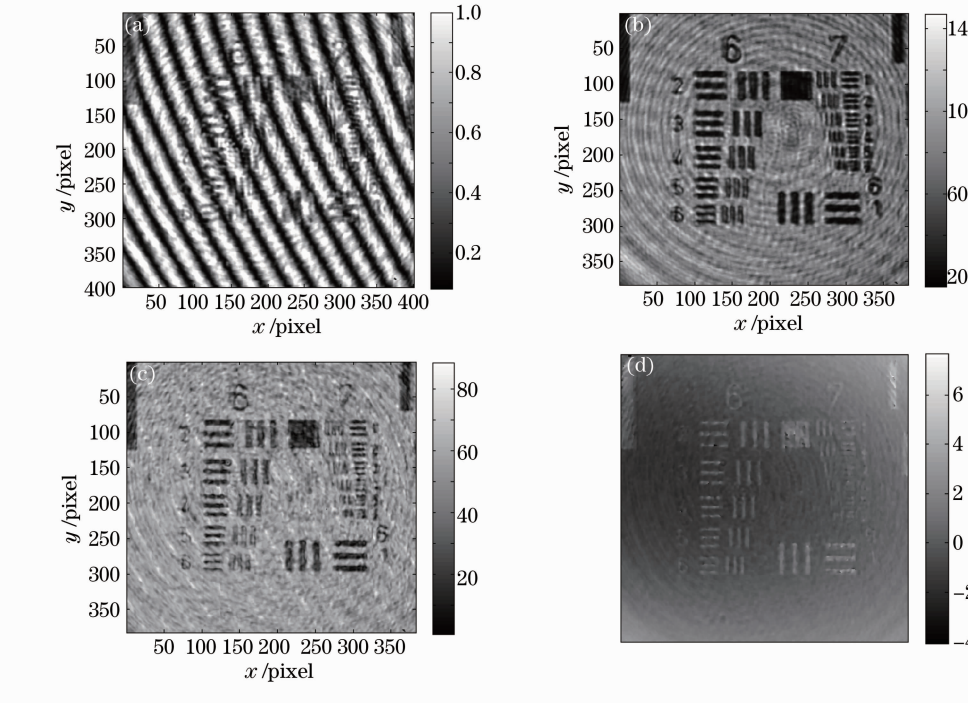

Fig. 7 Experimental data acquired by traditional Linik interferometer. (a) One of four holograms; (b) recorded intensity distribution of object wave with blocking the reference beam; (c) reconstructed intensity distribution by self-calibration phase-shifting method; (d) reconstructed unwrapped phase distribution

distribution with blocking the reference beam and the reconstructed one. Figure 6 shows the intensity distributions of object wave. The reconstructed intensity distribution of object wave by self-calibration four-step phase-shifting scheme is better than the reconstructed one by traditional four-step phase-shifting holography visually. The latter one has obvious fringe pattern, which is caused by the incomplete subtraction of Eq. (3). After performing the operation of Eq. (11), we can obtain their correlation coefficients. The

traditionally reconstructed one is 0.7969, which is less than the self-calibration one 0.8792. So the self-calibration phase-shifting digital holographic microscopy has a good immunity to incorrect phase shifter calibration and ambient vibrations.

To verify that the improved Linik interferometer has a better reconstruction quality than traditional one, experimental results acquired in the traditional Linik interferometer setup are shown in Fig. 7. Figure 7(a) is the one of four holograms. Figure 7(b) is the recorded that some parasitic fringes exist in Fig. 7(b), which is caused by the interference among reflected light of the lens in Fig. 1(a).

5 Conclusion

We proposed a self-calibration phase-shifting digital holographic microscopy. With the use of improved Linik interferometer, the self-calibration phase-shifting has a better reconstruction quality, which is proved by the experimental results. In addition, this method needs to introduce and know the carrier frequency accurately. So it is suitable for the object with a smooth surface, such as a semiconductor chip or microstructure devices with a flat substrate. For the object with a rough surface, this method is not suitable.

References

1 C J Mann, L F Yu, M K Kim. High-resolution quantitative phase-contrast microscopy by digital holography [J]. Opt Express, 2005, 13(22): 8693 - 8698.

2 P S Carney, J C Schotland. Three-dimensional total internal reflection microscopy [J]. Opt Lett, 2001, 26(14): 1072 - 1074.

3 W M Ash, M K Kim. Digital holography of total internal reflection intensity distribution of object wave with blocking the reference beam. Figures 7(c) and (d) are the reconstructed intensity and phase distributions by the self-calibration method proposed in this paper. The clearness of reconstructed wave-front intensity distribution degrades greatly. And its correlation coefficient is 0.7479, which is smaller than the one obtained in improved Linik interferometer. So the improved Linik interferometer can improve reconstruction resolution obviously. It should be noted [J]. Opt Express, 2008, 16(13): 9811 - 9820.

4 F Charrière, J Kühn, C Depeursinge. Characterization of microlenses by digital holographic microscopy [J]. Appl Opt, 2006, 45(5): 829 - 835.

5 T Colomb, S Krivec, Y Emery. Digital holographic reflectometry [J]. Opt Express, 2010, 18(4): 3719 - 3731.

6 I-B Kong, S-W Kim. General algorithm of phase-shifting interferometry by iterative least-squares fitting [J]. Opt Eng, 1995, 34(1): 183 - 188.

7 S-W Kim, M-G Kang, G-S Han. Accelerated phase-measuring algorithm of least squares for phase-shifting interferometry [J]. Opt Eng, 1997, 36(11): 3101 - 3106.

8 J Vargas, J A Quiroga, T Belenguer. Phase-shifting interferometry based on induced vibrations [J]. Opt Express, 2011, 19(2): 584 - 596.

9 K A Goldberg, J Bokor. Fourier-transform method of phase-shift determination [J]. Appl Opt, 2001, 40(17): 2886 - 2894.

10 T Zhang, I Yamaguchi. Three-dimensional microscopy with phase-shifting digital holography [J]. Opt Lett, 1998, 23(15): 1221 - 1223.

11 I Yamaguchi, T Ida, M Yokota, *et al*.. Surface shape measurement by phase-shifting digital holography with a wavelength shift [J]. Appl Opt, 2006, 45(29): 7610 - 7616.

12 Yi Qin, Jingang Zhong. Quality evaluation of phase reconstruction in LED-based digital holography [J]. Chin Opt Lett, 2009, 7(12): 1146 - 1150.

栏目编辑: 宋梅梅